

## Supporting Information

### **Piezoelectric Built-in Electric Field Advancing TiO<sub>2</sub> for Highly Efficient Photocatalytic Air Purification**

Mengmeng Li<sup>a,†</sup>, Qin Cheng<sup>a,†</sup>, Cheng Shen<sup>a</sup>, Bin Hong<sup>b</sup>, Yong Jiang<sup>c</sup>, Yuxue Wei<sup>a</sup>,  
Mengdie Cai<sup>a</sup>, Jingshuai Chen<sup>a</sup>, Song Sun<sup>a\*</sup>

<sup>a</sup> School of Chemistry and Chemical Engineering, Anhui University, Hefei, Anhui  
230601, P. R. China

<sup>b</sup> Hefei Innovation Research Institute, Beihang University, Hefei, Anhui 230013, P. R.  
China

<sup>c</sup> Shanghai Synchrotron Radiation Facility, Zhangjiang National Laboratory, Shanghai  
Advanced Research Institute, Chinese Academy of Sciences, Shanghai 201204, P. R.  
China

### **Table of Contents**

1. Experimental details	S1
2. Photocatalytic activity test under UV irradiation	S1
3. In-situ DRIFTS	S2
4. Reference	S24

## **Experimental details**

All the chemicals were used as received without any further purification. Polyvinylidene fluoride, PVDF, MW~543000, (Macklin) (Hefei Hengji Technology Co., Ltd), N, N-Dimethylformamide (DMF) (Macklin) (Hefei Hengji Technology Co., Ltd).

During the hot-stretching process, the degree of polarization of the hybrid film S-TiO<sub>2</sub>/PVDF-n (n=1,2,3) can be controlled by changing the stretching ratio, n represents different stretching ratios.

Due to the current limitations of the tensile instrument made the stretch of photocatalysts have a limitation of width. Therefore, we used the method of weave, a certain number of tensile scales of the same strip catalysts together, the preparation of the catalyst did not change the catalyst ratio surface area and other factors for active testing in Schematic 1.



**Schematic 1**

## **Photocatalytic activity test under UV irradiation**

To confirm the polarization field ability of reactive oxygen species generated from

TiO<sub>2</sub>/PVDF, the activity of the samples for the photocatalytic degradation of gaseous formaldehyde and toluene were investigated by a homemade setup, which consists of a gas feed system, a photoreactor and an analytical system. The photocatalytic activity was tested using a 400 mL quartz photoreactor. The sample was placed in a suitable photoreactor. The gaseous formaldehyde/toluene and water vapor feed were obtained by bubbling 20 vol% O<sub>2</sub>/N<sub>2</sub> compressed air through the saturators containing formaldehyde/toluene and distilled water at 298 K, respectively. The light source employed for the photocatalytic reaction was a 300 W Xe-arc lamp (PLS-SXE300UV, Beijing Perfect light Technology Co., Ltd.) equipped with an IR-cutoff filter for eliminating the thermal effect. The irradiation intensity at 365 nm on the photocatalyst surface was 215 mW/cm<sup>2</sup>. Before the reaction, the sample was kept in the dark for 20 min to reach the adsorption/desorption equilibrium on the photocatalyst surface. The formaldehyde/toluene concentration in the photoreactor was analyzed by a gas chromatograph (GC1690, Hangzhou Kexiao Scientific Instruments Co., Ltd.) equipped with a flame ionization detector (FID) and a chromatographic column (KX-112, Lanzhou Institute of Chemical Physics). The initial formaldehyde concentration was 100 ppmV and toluene concentration was 50 ppmV.

### **In-situ DRIFTS**

For in-situ diffuse reflectance infrared Fourier transform spectroscopy (DRIFTS) experiments, a Bruker IFS 66 v/s Fourier transform infrared spectrometer (FTIR) spectromete equipped with a deuterated triglycine sulfate (DTGS) detector was used and operated under OPUS/IR software. A reaction system, consisting of a praying

mantis DRIFT spectra accessory (Harrick Scientific) and a reaction cell (HVC, Harrick Scientific) was employed. The reaction cell was equipped with a heater and housed a sample cup for the photocatalysts. A dome with three windows covered the sample cup and was maintained in place with retaining plates. Two of the IR transparent windows were made of KBr, while the third was made of quartz to allow the photocatalyst to be irradiated by UV light. The same light source used in the photocatalytic activity test was adopted for irradiation. In the experiment, the reactants entered and exited the cell through a set of inlet and outlet ports. The reaction gas flow rate was 10 sccm. In-situ DRIFT spectra of formaldehyde adsorption and photocatalytic degradation were collected in the range of 4000-650  $\text{cm}^{-1}$  by averaging 4 scans with a resolution of 4  $\text{cm}^{-1}$  at a scanning velocity of 10 kHz. A detailed account of the experimental setup has been reported elsewhere.<sup>1,2</sup>

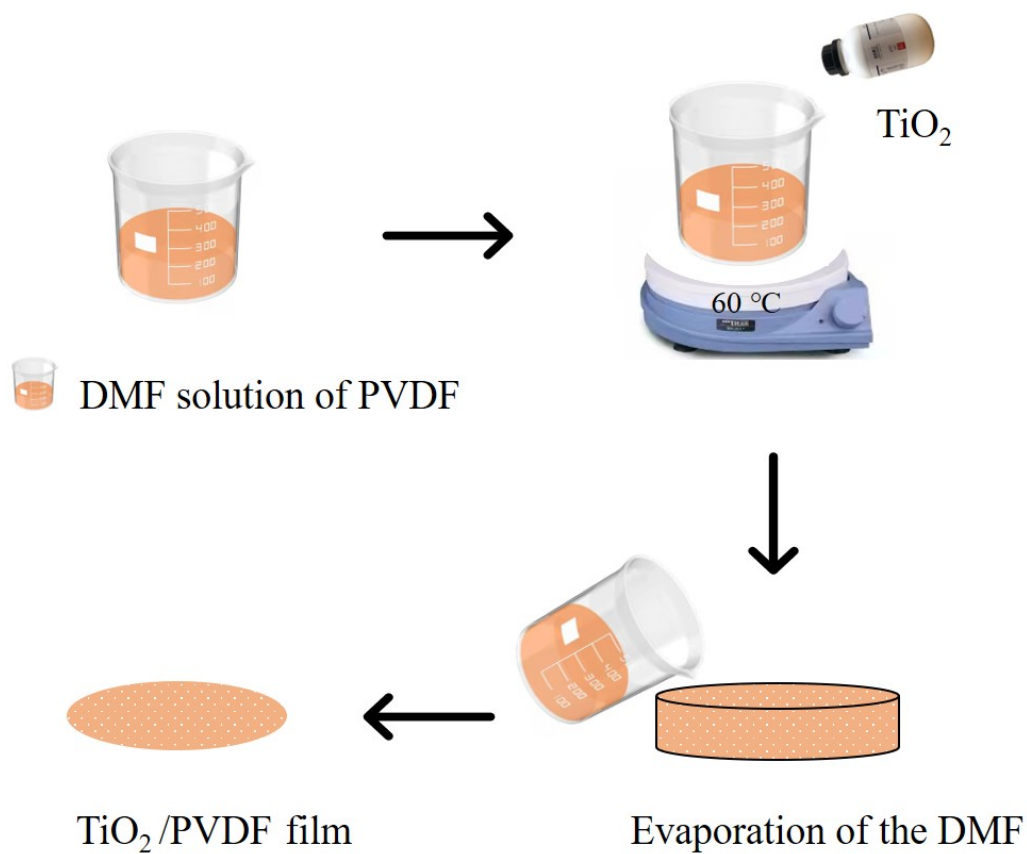


**Fig. S1** Preparation schematic for TiO<sub>2</sub>/PVDF film.

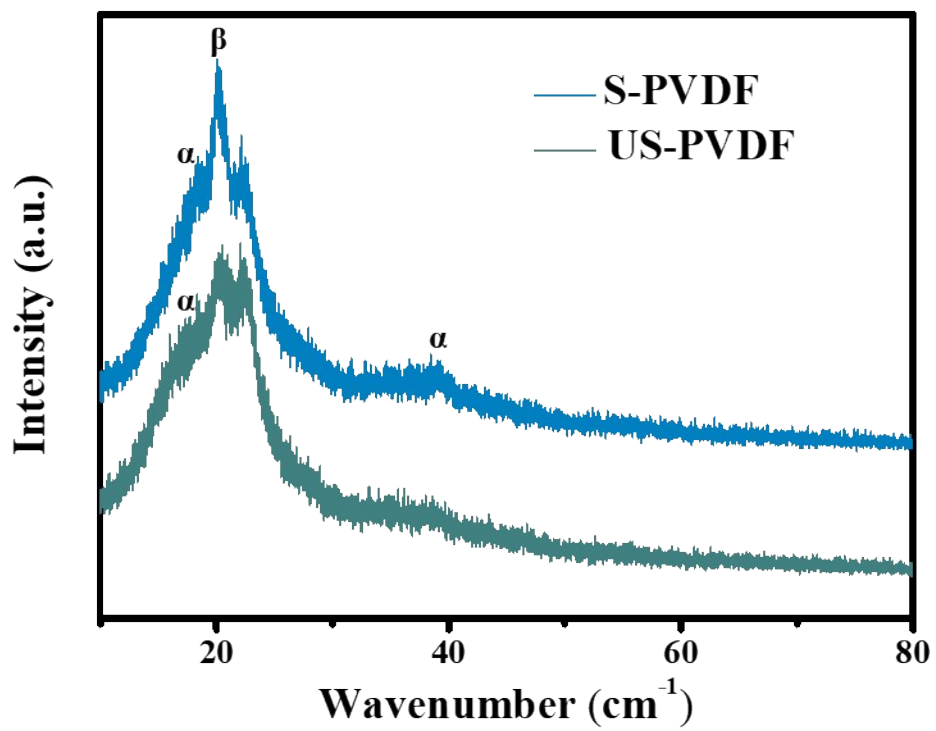
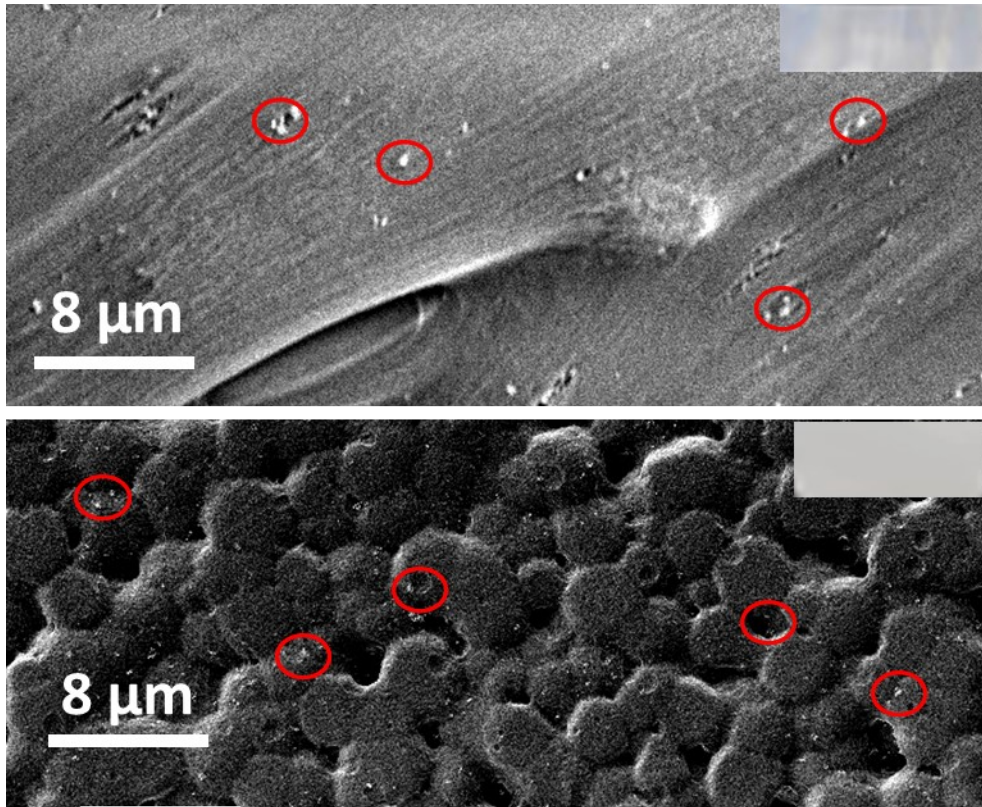
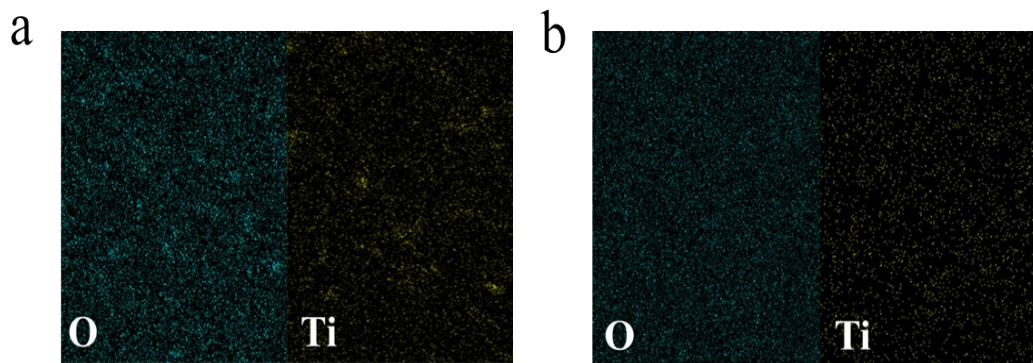


Fig. S2 XRD of PVDF film.



**Fig. S3** SEM images of US-TiO<sub>2</sub>/PVDF (up) and photograph of US-TiO<sub>2</sub>/PVDF (inset), S-TiO<sub>2</sub>/PVDF (down) and photograph of S-TiO<sub>2</sub>/PVDF (inset). The ones in the red circle are TiO<sub>2</sub>.



**Fig. S4** SEM elemental mapping of (a) US-TiO<sub>2</sub>/PVDF and (b) S- TiO<sub>2</sub>/PVDF.



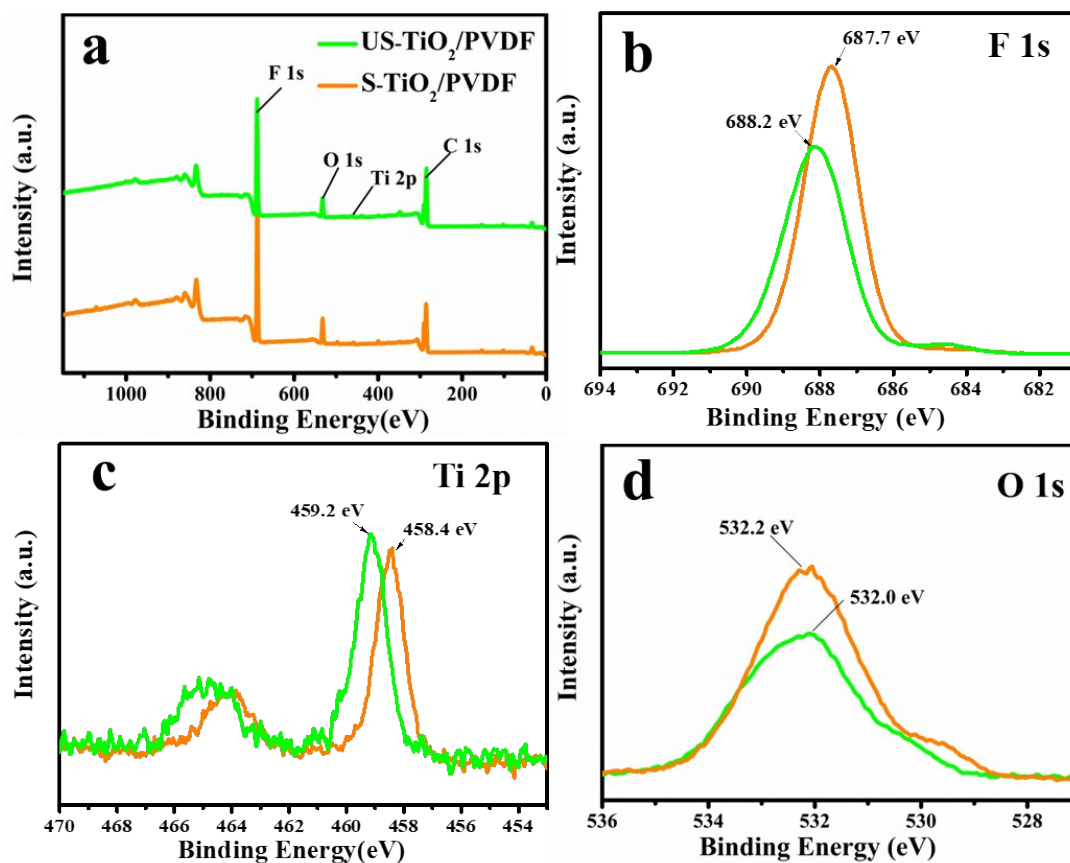


**Fig. S5** (a) Survey XPS spectra of US-TiO<sub>2</sub>/PVDF and S-TiO<sub>2</sub>/PVDF. (b) F 1s, (c) Ti 2p and (d) O 1s XPS spectra of US-TiO<sub>2</sub>/PVDF and S-TiO<sub>2</sub>/PVDF.

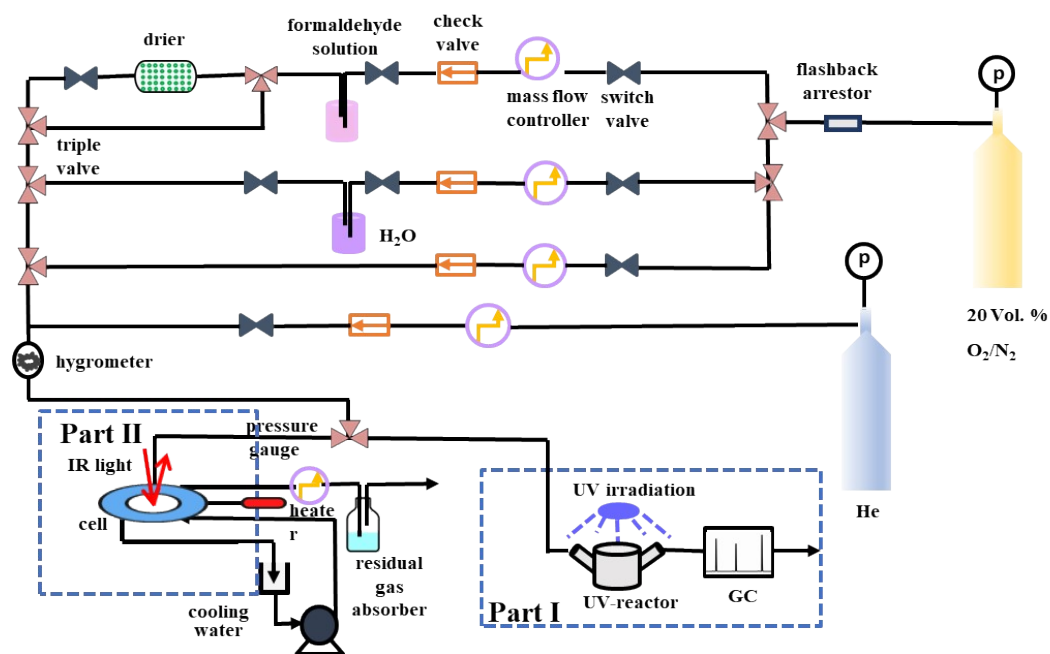


**Fig. S6** Homemade setup consists of a gas feed system, a photoreactor and an analytical system.

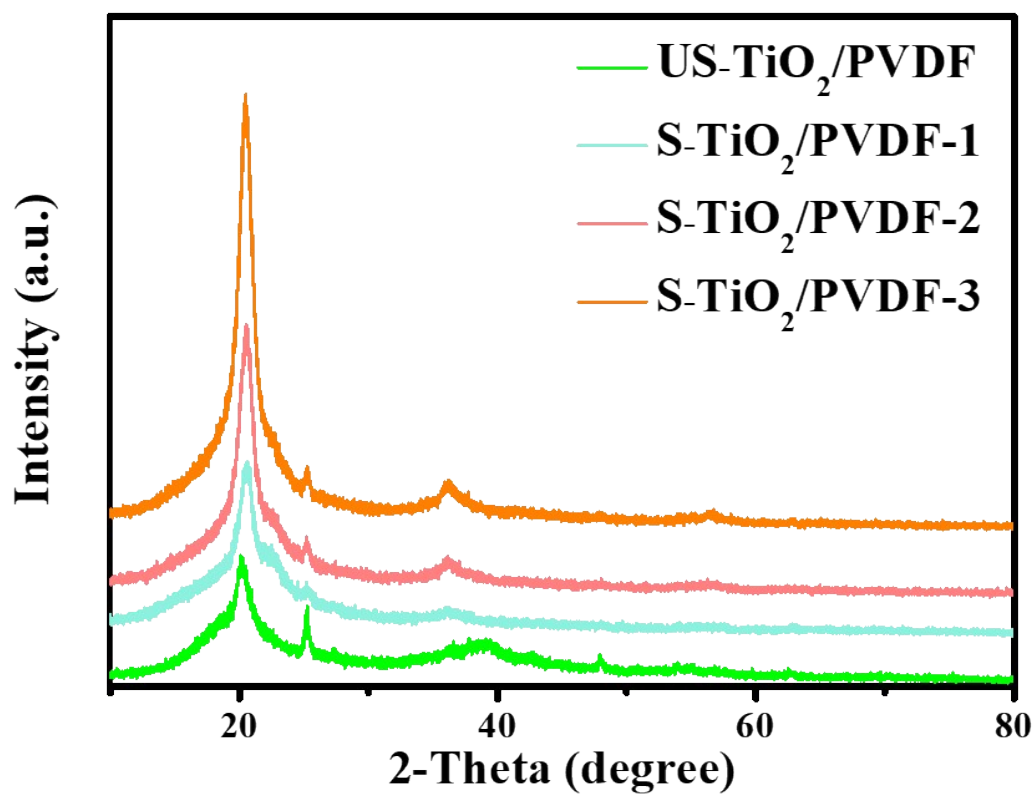


**Fig. S7** XRD of different tensile ratios TiO<sub>2</sub>/PVDF film.

During the hot-stretching process, the degree of polarization of the hybrid film S-TiO<sub>2</sub>/PVDF-n (n=1,2,3) can be controlled by changing the stretching ratio, n represents different stretching ratios, such as n=1 means the stretched length is double the original length.

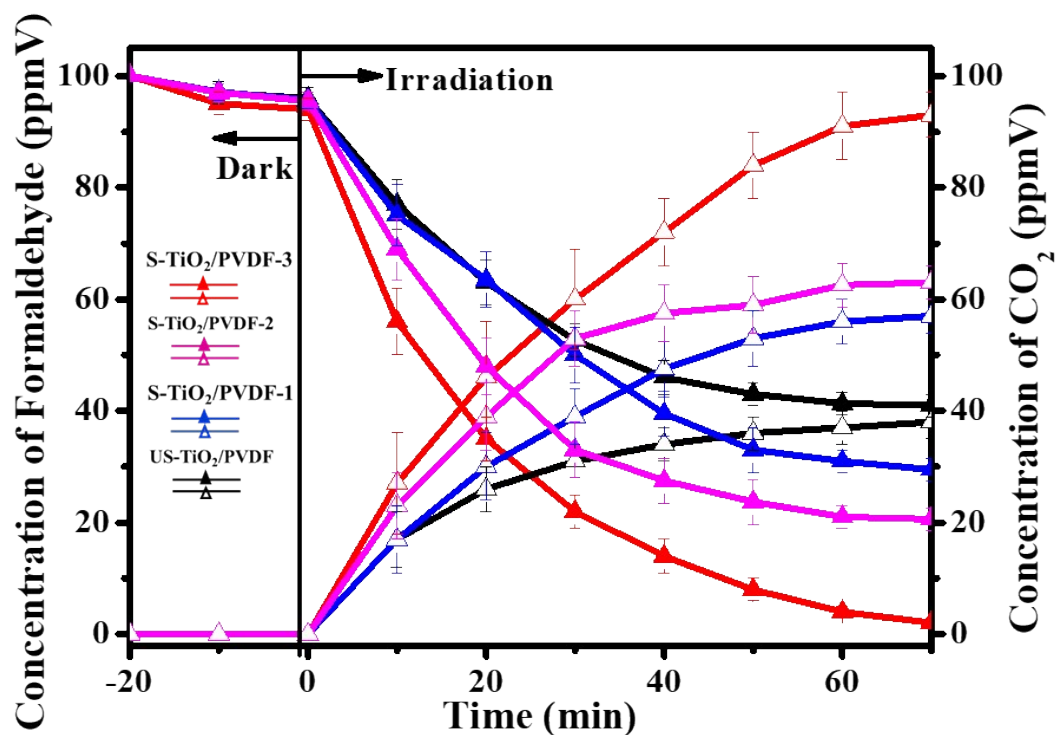


**Fig. S8** Photocatalytic performance of samples. Reaction condition: formaldehyde initial concentration: 100 ppmV; light source: 300 W xenon lamp; R.H.: 70%; Temperature: 298 K. Solid and open symbols represent the concentration of formaldehyde and the concentration of CO<sub>2</sub> generated by the degradation of formaldehyde, respectively.

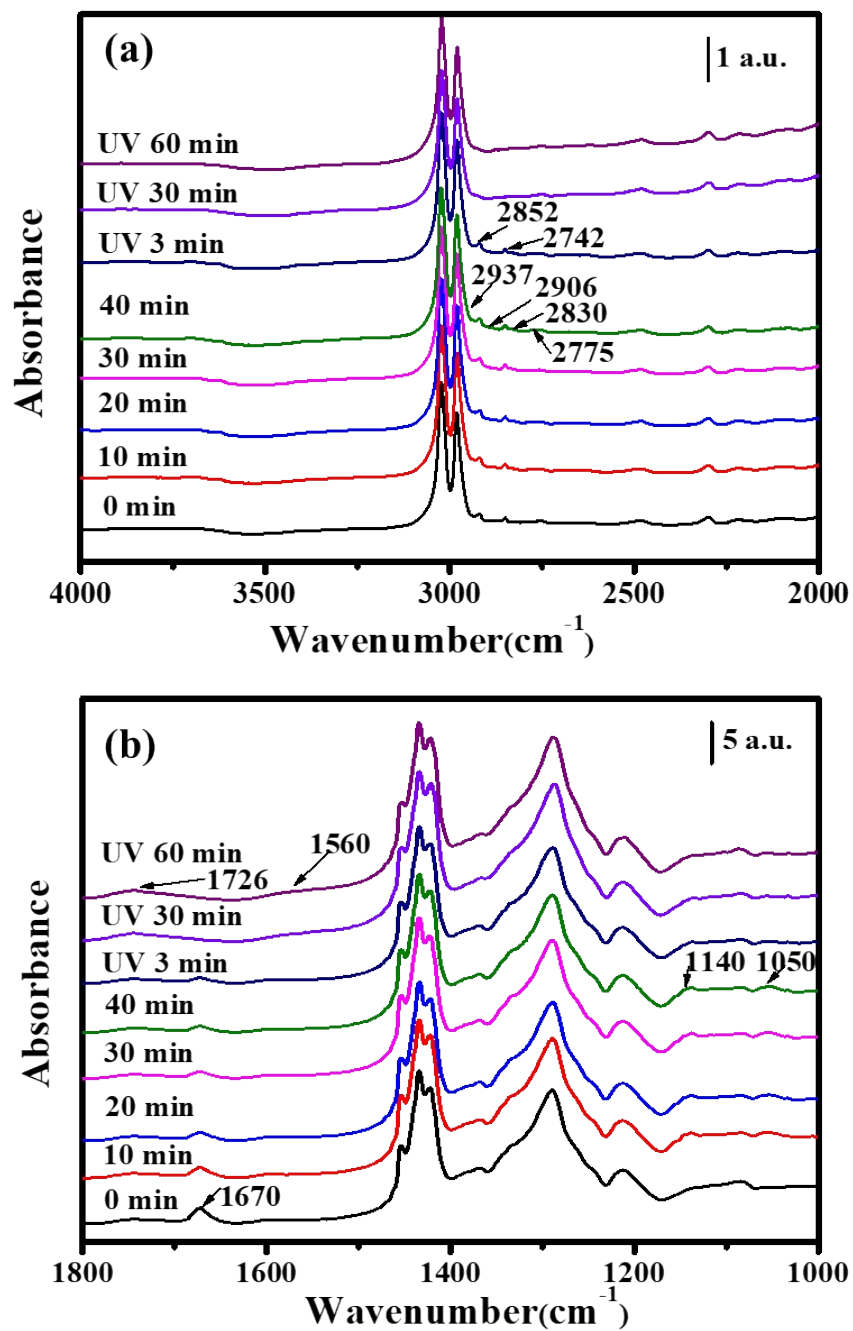


**Fig. S9** In-situ DRIFT spectra for the absorption of formaldehyde and with UV irradiation after achieving absorption equilibrium on US-TiO<sub>2</sub>/PDVF.

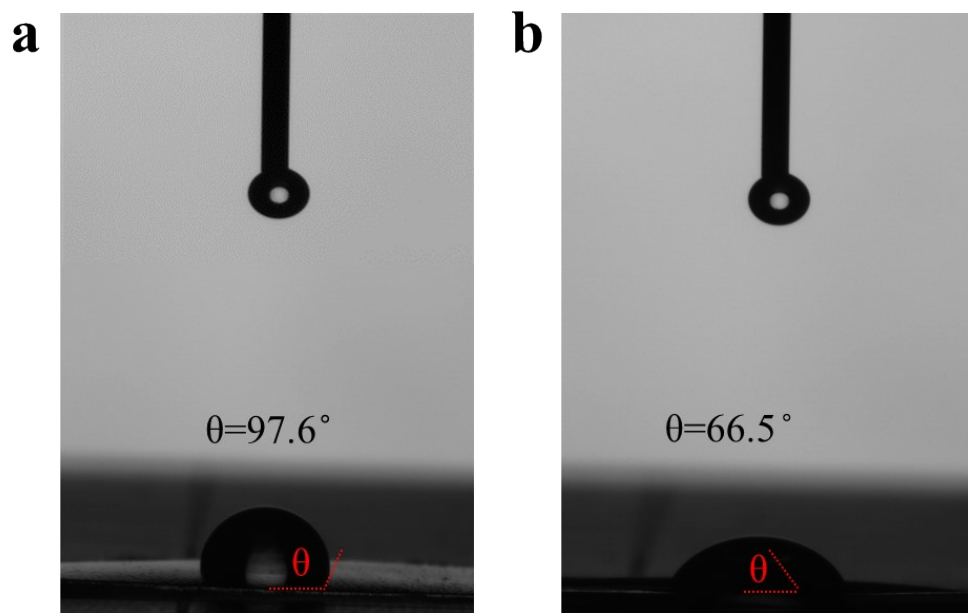


**Fig. S10** Contact angle measurement of (a) US-TiO<sub>2</sub>/PVDF and (b) S-TiO<sub>2</sub>/PVDF.

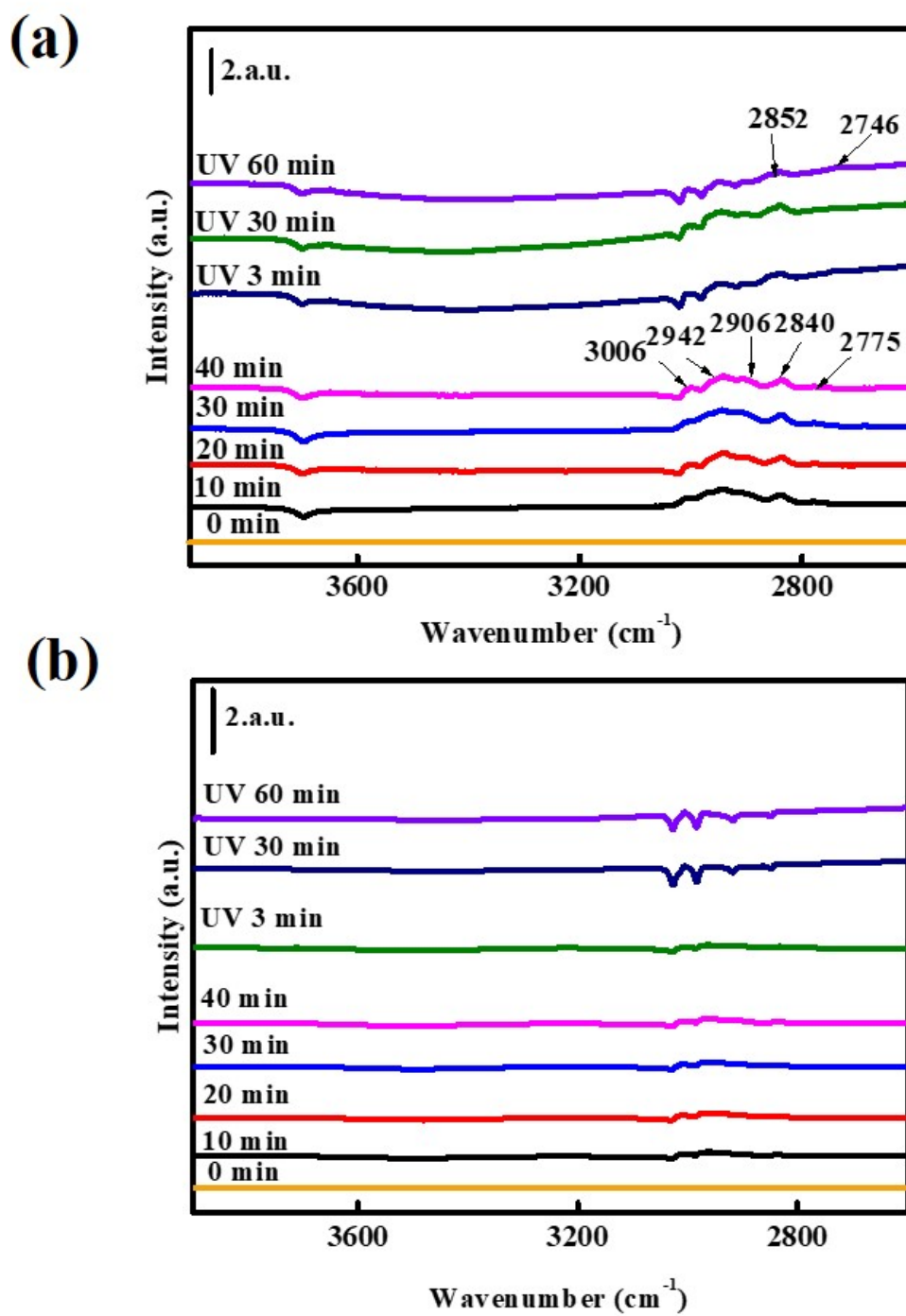


**Fig. S11** FTIR difference spectrum of formaldehyde absorption and UV irradiation on US-TiO<sub>2</sub>/PVDF.

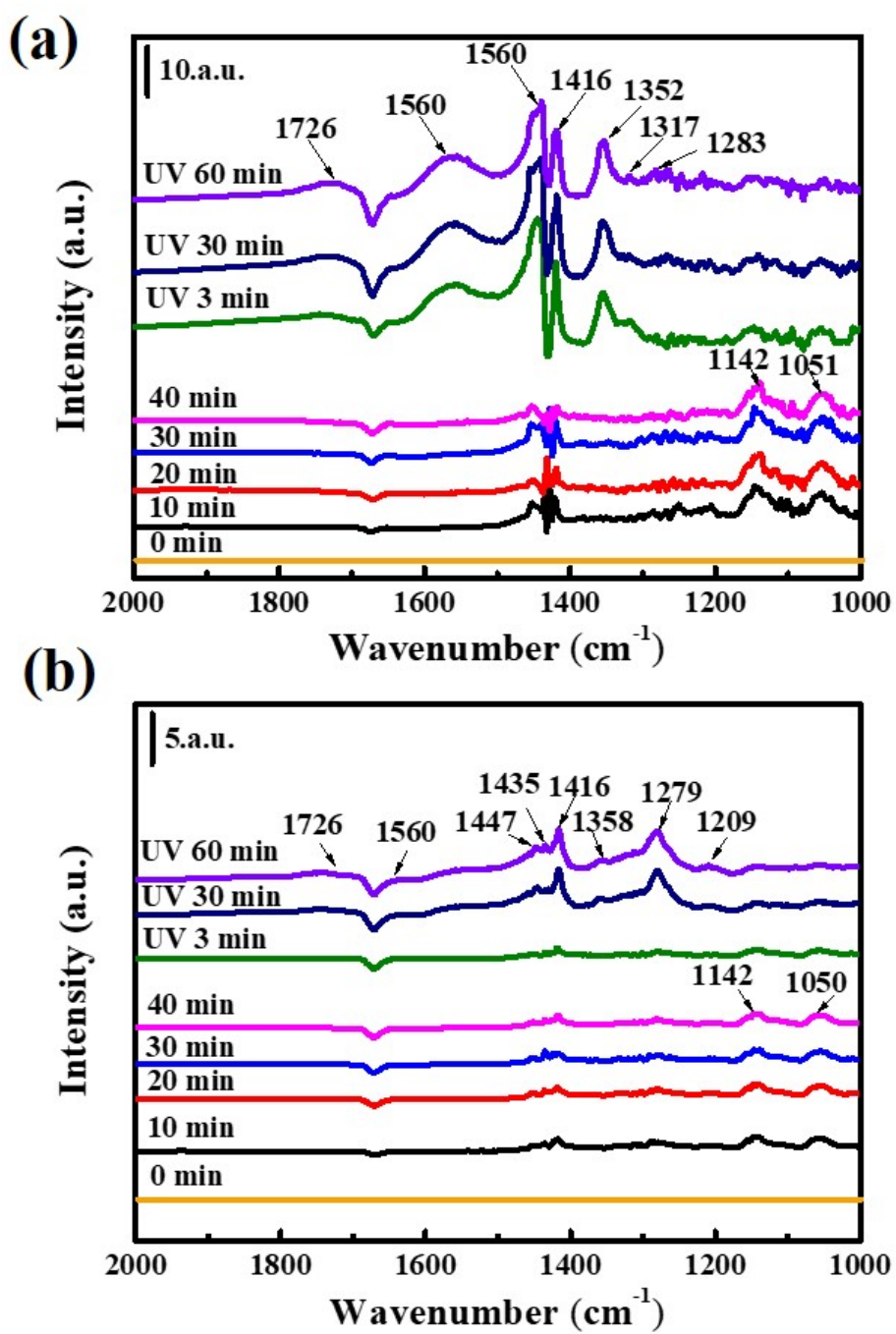


**Fig. S12** FTIR difference spectrum of formaldehyde absorption and UV irradiation on US-TiO<sub>2</sub>/PVDF.



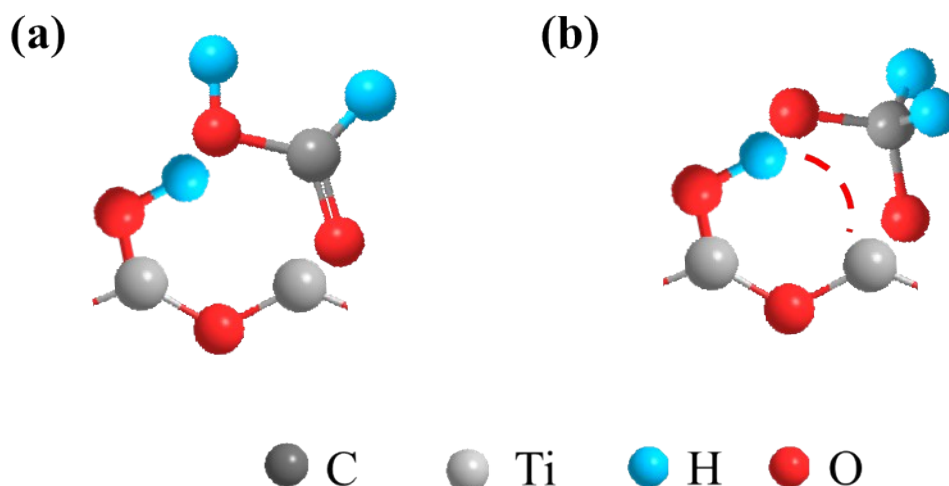


**Fig. S13** The intermediate adsorption states during degradation process on (a) S-TiO<sub>2</sub>/PVDF, and (b) US-TiO<sub>2</sub>/PVDF.

After the hybrid film was stretched, the dipole moment of PVDF increased and the H (+) and F (-) atoms were arranged in rows (Fig. 1a), thus changing the electronegativity of TiO<sub>2</sub> on the film surface (Fig. 4), so that S-TiO<sub>2</sub>/PVDF surface hydroxyl adsorption was enhanced, and the polarization field promoted the separation of charges, the rapid charge of the offensive surface adsorption hydroxyl, oxygen molecules etc., these •OH and •O<sub>2</sub><sup>-</sup> adsorptions or freeness adsorption on the surface of the film's surface attack formaldehyde, therefore these intermediates were mainly in the form of formate on S-TiO<sub>2</sub>/PVDF. While on US-TiO<sub>2</sub>/PVDF, due to the lack of these •OH and •O<sub>2</sub><sup>-</sup>, these intermediates could not be consumed in time and accumulated on the surface of the catalyst, therefore these intermediates were mainly in the form of DOM on US-TiO<sub>2</sub>/PVDF (Fig. S13b).<sup>3</sup>

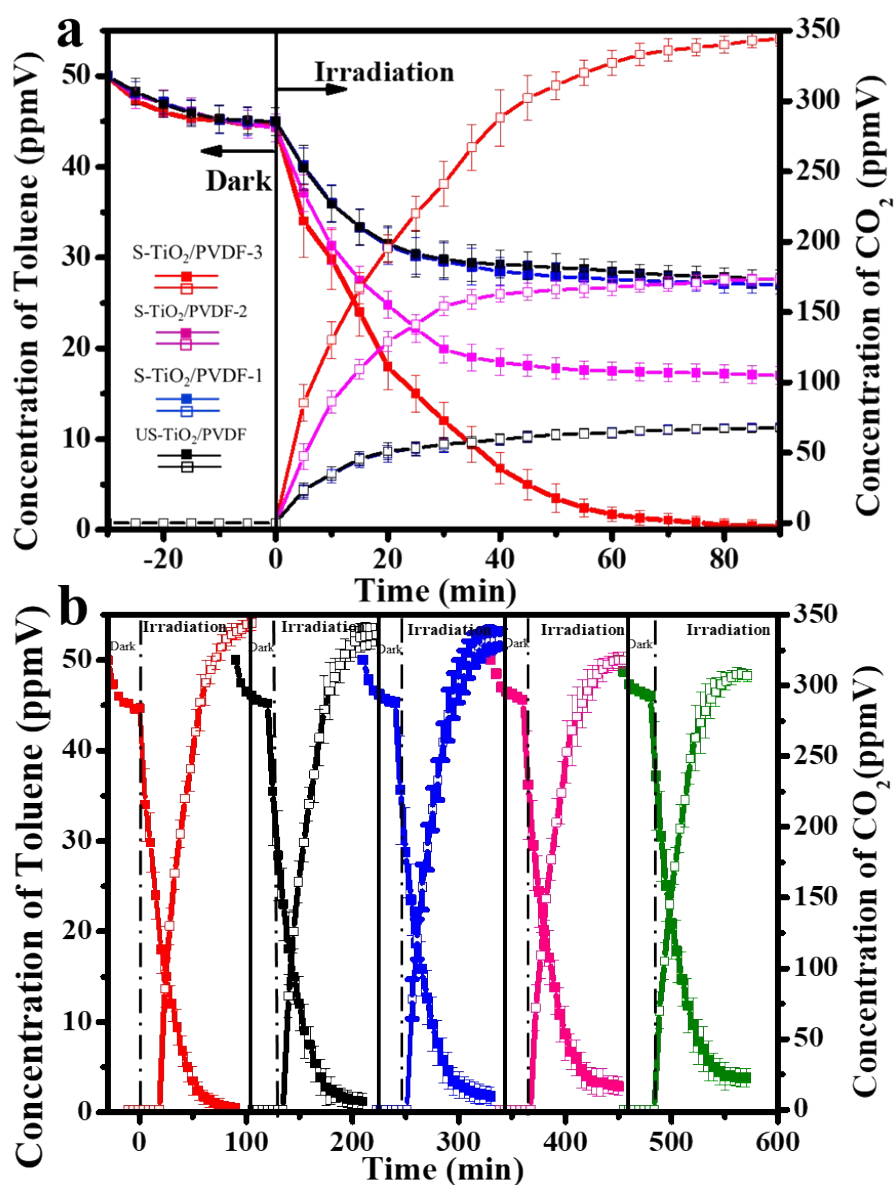


**Fig. S14** (a) Photocatalytic performance of samples. Reaction condition: toluene initial concentration: 50 ppmV; light source: 300 W xenon lamp; R.H.: 70%; Temperature: 298 K. (b) Stability test of S-TiO<sub>2</sub>/PDVF for repeated photocatalytic degradation of with an initial concentration of 50 ppmV. Solid and open symbols represent the concentration of toluene and the concentration of CO<sub>2</sub> generated by the degradation of toluene, respectively.

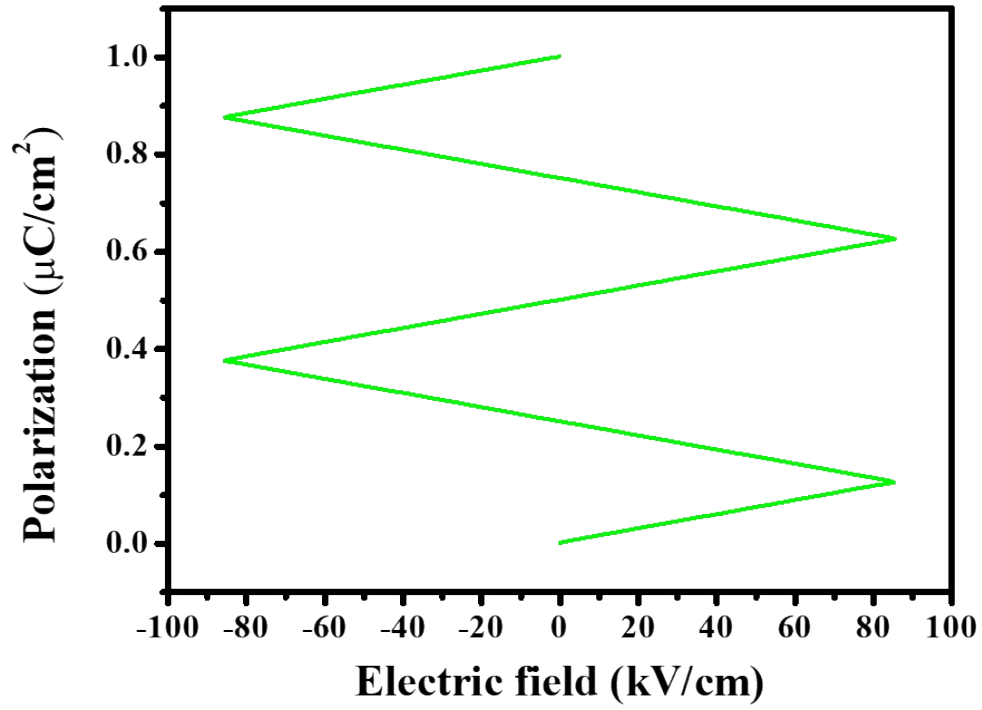


**Fig. S15** Electric hysteresis loop for US-TiO<sub>2</sub>/PVDF.

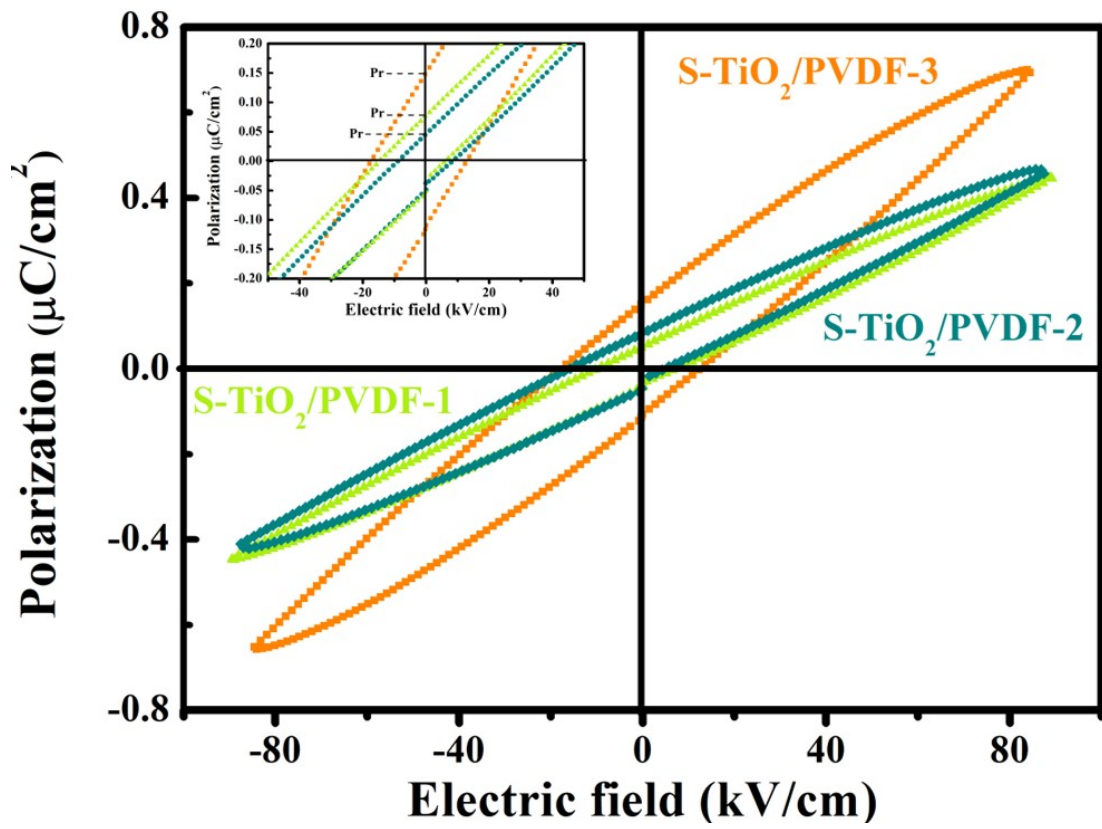
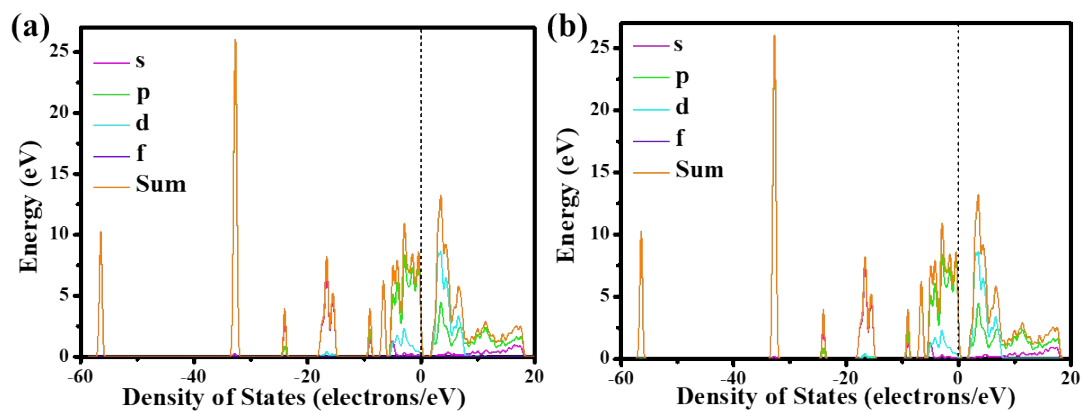
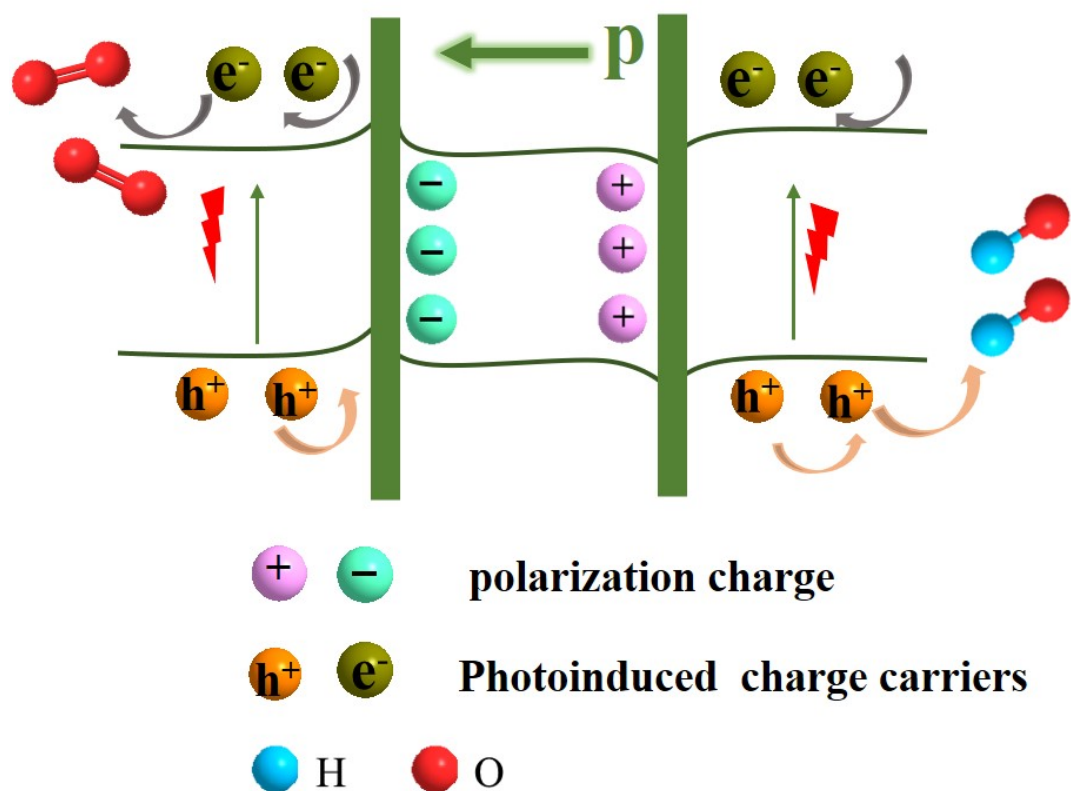


Fig. S16 Electric hysteresis loops of different tensile ratios TiO<sub>2</sub>/PVDF film and magnified image (inset).



**Fig. S17** Density of states (DOS) of (a) TiO<sub>2</sub> without polarization field, and (b) TiO<sub>2</sub> with polarization field.



**Fig. S18** A diagram of the mechanism of polarization field promotes the separation charge.

**Table S1.** Bands (in  $\text{cm}^{-1}$ ) observed in the formaldehyde and their possible assignments.

Assignment	Frequency/ $\text{cm}^{-1}$
$\nu(\text{O-H})$	3700
$\nu_{\text{as}}(\text{C-H})$	2940-2950
$\nu(\text{C-H})$	2906
$\nu_{\text{as}}(\text{C-H})$	2840-2830
$\nu_{\text{s}}(\text{C-H})$	2775
$\delta(\text{H-O-H})$	1670
POM	1142
P(C-H)	1108
HCHO	1051

**Table S2.** Bands (in  $\text{cm}^{-1}$ ) observed in the formate and their possible assignments.

Assignment	Frequency/ $\text{cm}^{-1}$
$\nu(\text{C-H})$ in formate	2852
$\nu_s(\text{OCO}) + \nu(\text{CH})$ in formate	2746
$\nu(\text{CO})$ in $\text{HCOO}^-$	1715-1730
$\nu_a(\text{OCO})$	1560
$\nu(\text{CH}_2)$	1447-1440
$\nu(\text{OCO})$ in DOM	1416
$\nu_s(\text{OCO})$	1352
$\tau(\text{CH}_2)$	1318
$\tau(\text{CH}_2)$	1283-1275
POM	1209



## Reference

- 1 F. Zhang, M. Wang, X. Zhu, B. Hong, W. Wang, Z. Qi, W. Xie, J. Ding, J. Bao, S. Sun and C. Gao, *Appl. Catal. B.*, 2015, **170**, 215-224.
- 2 S. Sun, F. Zhang, Z. Qi, J. Ding, J. Bao and C. Gao, *ChemCatChem.*, 2014, **6**, 2535-2539.
- 3 T. Kecskés, J. Raskó and J. Kiss, *Appl.Catal. A.*, 2004, **273**, 55-62.